Journal of
Composites Science

MDPI

Article

Interactions of Cd^{2+}, Co^{2+} and MoO_4^{2-} Ions with Crushed Concrete Fines

Victoria K. Elmes and Nichola J. Coleman *

Faculty of Engineering and Science, University of Greenwich, Chatham Maritime, ME4 4TB Kent, UK; v.elmes@gre.ac.uk
* Correspondence: n.coleman@gre.ac.uk

Abstract: Construction and demolition activities generate approximately two thirds of the world's waste, with concrete-based demolition material accounting for the largest proportion. Primary aggregates are recovered and reused, although the cement-rich fine fraction is underutilised. In this study, single metal batch sorption experiments confirmed that crushed concrete fines (CCF) are an effective sorbent for the maximum exclusion of 45.2 mg g^{-1} Cd^{2+}, 38.4 mg g^{-1} Co^{2+} and 56.0 mg g^{-1} MoO_4^{2-} ions from aqueous media. The principal mechanisms of sorption were determined, by scanning electron microscopy of the metal-laden CCF, to be co-precipitation with Ca^{2+} ions released from the cement to form solubility limiting phases. The removal of Co^{2+} and MoO_4^{2-} ions followed a zero-order reaction and that of Cd^{2+} was best described by a pseudo-second-order model. The Langmuir model provided the most appropriate description of the steady state immobilisation of Cd^{2+} and Co^{2+}, whereas the removal of MoO_4^{2-} conformed to the Freundlich isotherm. Long equilibration times (>120 h), loose floc formation and high pH are likely to limit the use of CCF in many conventional wastewater treatment applications; although, these properties could be usefully exploited in reactive barriers for the management of contaminated soils, sediments and groundwater.

Keywords: recycled; aggregate; cement; construction and demolition waste; cadmium, cobalt, molybdenum, heavy metals, sorbent

Citation: Elmes, V.K.; Coleman, N.J. Interactions of Cd^{2+}, Co^{2+} and MoO_4^{2-} Ions with Crushed Concrete Fines. *J. Compos. Sci.* **2021**, *5*, 42. https://doi.org/10.3390/jcs5020042

Received: 11 January 2021
Accepted: 27 January 2021
Published: 1 February 2021

1. Introduction

Construction and demolition (C&D) waste represents approximately two thirds of the world's refuse [1,2]. Of this, concrete-based demolition material accounts for the largest proportion, estimated to be between 75 and 88%, with the USA, China and Europe generating 320 Mt, 240 Mt and 510 Mt, respectively, per annum [3,4]. After water, concrete is the second most consumed resource with a global production of around one tonne per person per annum (~3.8 billion cubic metres), which will inevitably enter the C&D waste stream in the future [5].

In order to conserve natural resources and divert C&D waste from landfill, various national and regional directives have been set up to encourage more recycling within the construction industry. For example, the European Waste Framework Directive 2008/98/EC set a target for the recycling of 70% of C&D waste by 2020, which many member states failed to achieve [6–8]. In the USA, the Resource Conservation and Recovery Act empowers the Environmental Protection Agency (EPA) to promote and regulate the recycling of C&D waste, although approximately one quarter of all C&D debris was consigned to landfill in 2018 [9].

Concrete is a composite comprising a hydrated cement matrix embedded with 'aggregates' of sand, gravel and crushed rock. The mechanical crushing, sieving and sorting of concrete-based demolition waste, for the recovery and reuse of the aggregates, produces a large volume of fine (<5 mm), low-density, cement-rich material for which further market development is required [7,10,11]. In this respect, a number of recent studies has been carried out that seek to exploit the porous, absorbent and alkaline nature of the

cement-rich fine material in the treatment of contaminated water [1,3,5,6,10,12–23] and marine sediment [24–26]. Crushed concrete fines (CCF) are reported to be effective in the removal of various heavy metal species (AsO_3^{3-} [12], CrO_4^{2-} [12], $H_nPO_4^{(3-n)-}$ [20–23], Cd^{2+} [13–15], Cu^{2+} [10,13,17,18], Ni^{2+} [13], Pb^{2+} [10,13,15,16,18], Zn^{2+} [10,13,18]), radionuclides ($^{60}Co^{2+}$ [1,5,6], $^{63}Ni^{2+}$ [1,5,6], $^{90}Sr^{2+}$ [1,5,6], $^{85}Sr^{2+}$ [19], $^{223}Ra^{2+}$ [19]) and organic dyes (disperse red and reactive brilliant blue [3]) from aqueous solutions. CCF have also been proposed as components in permeable reactive barriers for the sequestration of Pb^{2+}, Cu^{2+}, Ni^{2+} and Fe^{2+} ions from groundwater at landfill sites [27,28].

Mature hydrated Portland cement is principally composed of ~70 wt% nonstoichiometric nanoporous calcium silicate hydrate (C-S-H) gel matrix, ~20–30 wt% hexagonal crystals of calcium hydroxide (aka portlandite,) and minor quantities of various calcium aluminate hydrate phases (e.g. ettringite (AFt, $6CaO{\cdot}Al_2O_3{\cdot}3SO_3{\cdot}32H_2O$), monosulphate (AFm, $4CaO{\cdot}Al_2O_3{\cdot}SO_3{\cdot}13H_2O$), tetracalcium aluminate hydrate ($4CaO{\cdot}Al_2O_3{\cdot}13H_2O$) and hydrotalcite ($6MgO{\cdot}Al_2O_3{\cdot}CO_2{\cdot}12H_2O$)) depending on the age of the cement [29]. All of the phases are impure (i.e., substituted with guest ions) and become progressively carbonated via exposure to atmospheric carbon dioxide which also gives rise to calcium carbonate within the cement matrix. Residual water within the porous cement system is highly alkaline (typically pH > 12.5) by virtue of dissolved alkali metals and calcium ions. On exposure to acidic environments, the high pH is buffered by the dissolution of portlandite which affords the cement a substantial acid-neutralising capacity (ANC) [14].

Aqueous heavy metals and radionuclides can be immobilised within the mature cement matrix by the pH-mediated precipitation of simple salts, and by co-precipitation and complex formation with constituents of the cement, thus forming solubility-limiting phases [30]. Metal ions can also be retained by chemi- and physisorption onto the surfaces of the cement phases, especially the high surface area nanoporous C-S-H gel. In addition, substitution into the existing lattices of the C-S-H gel, portlandite and calcium aluminate hydrate phases is possible, forming solid solutions and, in this respect, ettringite is particularly compliant to extensive substitution of both cations and oxyanions [30].

Cadmium is a non-essential carcinogenic heavy metal whose industrial applications include metal plating, alloys, pigments and batteries [29]. It exerts toxicity via a wide range of biological mechanisms and is associated with renal damage, osteoporosis and various cancers [31]. The aqueous chemistry of cadmium generally concerns the divalent cadmium (II) cation, $Cd^{2+}_{(aq)}$, although the diatomic monovalent cadmium (I) species, $Cd_2^{2+}{}_{(aq)}$, is also known.

Aqueous Cd^{2+} ions are reported to be immobilised in fresh cement paste by substitution into ettringite, C-S-H gel and portlandite [30], yet few studies have been carried out to determine the interactions of Cd^{2+} with aged cement. Shin et al. [13] demonstrated that mature 0.5–1.0 mm CCF can take up 0.27 mg g^{-1} of cadmium under batch conditions (10 ppm solution at solid:solution ratio 1.0 mg cm^{-3}), although the fate of the metal was not documented. The sorption capacity was found to increase to 0.61 mg g^{-1} on pre-treatment of the CCF with sodium hydroxide solution, indicating that the mechanism of retention was at least partly pH-mediated. A similar maximum sorption capacity of 0.294 mg g^{-1} was reported by Damrongsiri [14] for 0.063–2.0 mm CCF using a Langmuir isotherm to model Cd^{2+}-uptake (solid:solution ratio 25 mg cm^{-3}, with a maximum concentration of 4.0 ppm). Conversely, a significantly higher sorption capacity of 16.5 mg g^{-1} was reported for autoclaved aerated CCF exposed to solutions of up to 2000 ppm (solid:solution ratio 100 mg cm^{-3}), which was also obtained using the Langmuir model [15]. This research involved a comprehensive investigation of the kinetics and equilibrium uptake of Cd^{2+} ions but, again, the fate of the immobilised cadmium was not reported [15]. The superior sorption capacity of the autoclaved aerated cement may have arisen from the markedly higher concentration of the supernatant solutions, but may also be attributed to the crystalline nature of the major C-S-H phase in autoclaved cement (i.e., tobermorite), which is known to have a substantial ion-exchange capacity for Cd^{2+} ions (~180 mg g^{-1}) [32].

Cobalt is an essential element in all animal species and finds wide industrial application in alloys, catalysts, batteries and pigments [33]. The radionuclide ^{60}Co is a technologically significant isotope in medicine and food sterilisation, and it is also a constituent of the post-decommissioning liquid radioactive waste stream 20–30 years after reactor shutdown [1,5,6]. In humans, cobalt toxicity is associated with cardiomyopathy, hearing and sight impairment, hypothyroidism and various cancers [34].

Aqueous Co^{2+} ions are precipitated as hydroxides and silicates, incorporated into the ettringite phase and are also strongly sorbed to the C-S-H gel in fresh cement [30]. The common oxidation states of cobalt are (II) and (III) and the oxidation of Co^{2+} to Co^{3+} in fresh cement exposed to air has been reported [35]. Šljivić-Ivanović et al. [5] and Jelić et al. [6] investigated the uptake of Co^{2+} ions by 0.3–0.6 mm CCF from a 50-year-old demolished concrete pavement and found the maximum sorption capacity to be 18.9 mg g^{-1} under batch conditions (at solid:solution ratio 5 mg cm^{-3}, with a maximum concentration of 471 ppm). No morphological changes to the irregular agglomerates on the surface of the CCF grains were observed by scanning electron microscopy following exposure to a ternary solution of Co^{2+}, Ni^{2+} and Sr^{2+}, although energy dispersive X-ray analysis confirmed the presence of the three metals [5].

Molybdenum is an essential element in plants and animals; although, excessive intake can cause gout-like symptoms in humans and teart disease in cattle, which presents as anaemia, gastrointestinal disturbances and bone disorders [36,37]. The aqueous chemistry of molybdenum is complex, with the tetrahedral molybdate (VI), MoO_4^{2-}, anion existing in solution above pH 6, polymeric molybdate species forming between pH 4 and 6, and various protonated complexes occurring below pH 4 [36]. Molybdenum finds application in the chemical industries in catalysts, fertilisers, alloys, pigments, ceramics and lubricants, and the anthropogenic ^{99}Mo isotope is used extensively in diagnostic medical imaging [36].

On incorporation in fresh cement paste, the molybdate anion substitutes into the ettringite lattice and also forms the solubility limiting compound, powellite, $CaMoO_4$ [30]. A recent study has been carried out to investigate the uptake of the aqueous MoO_4^{2-} anion by 28-day hardened ordinary Portland cement paste and various individual hydrated cement phases under conditions that represent potential interactions between ^{93}Mo and cement in a nuclear waste repository [38]. Distribution coefficients, R_d, (i.e., the partition of Mo between the solid and solution phases at equilibrium) of 781, 1571, 122, 3037 and 789 L kg^{-1} were obtained for C-S-H gel, AFm, AFt, hydrogarnet and portlandite, respectively, under anoxic batch conditions in dilute (0.1–5.0 μM) MoO_4^{2-}-bearing liquors that had been pre-equilibrated with the cement phases [38]. The authors report that, MoO_4^{2-} underwent anion exchange into the AFm and AFt phases, was electrostatically sorbed to the C-S-H gel and precipitated as $CaMoO_4$ in the presence of portlandite. The hydrogarnet system was found to immobilise aqueous MoO_4^{2-} ions by dissolution and re-precipitation as a solubility limiting AFm-MoO_4 phase [38]. To date, the authors could not locate any studies in the literature concerning the interactions of molybdate compounds with crushed concrete-based demolition waste.

In the present study, the kinetics and equilibrium removal of Cd^{2+}, Co^{2+} and MoO_4^{2-} from aqueous solutions by the 1–2 mm fraction of CCF was investigated under batch sorption conditions. The metal-laden CCF granules were subjected to a distilled water leaching procedure to appraise the persistence of binding of the metal species. The surfaces and cross-sections of the metal-laden CCF granules were also analysed by scanning electron microscopy (SEM) and energy dispersive X-ray spectroscopy (EDX) to determine the fate of the bound metal species.

2. Materials and Methods

2.1. Preparation of Crushed Concrete Fines (CCF)

Laboratory-prepared CCF were selected for this study, rather than those obtained by crushed demolition waste, to provide a well-characterised, reproducible, uncontaminated sample against which the performance of real C&D waste can be evaluated in future

research. The CCF were obtained by crushing and grading a five-year-old concrete block, 0.4 × 0.4 × 0.3 m, prepared from 28.32 kg ordinary Portland cement (OPC) and sea-dredged flint aggregate (13.90, 44.22 and 43.87 kg of 5, 10, and 20 mm aggregate, respectively) at a water:cement ratio of 0.40. The block was broken with a hammer and chisel prior to jaw crushing and sieving out the 1–2 mm CCF fraction. The cement content of the CCF was determined to be 50.1 ± 0.4% (by nitric acid digestion).

2.2. Sorption of Cd^{2+}, Co^{2+} and MoO_4^{2-} by CCF

Evaluations of the kinetics of removal of Cd^{2+}, Co^{2+} and MoO_4^{2-} by CCF from single metal aqueous solutions of $Cd(NO_3)_2{\cdot}4H_2O$, $Co(NO_3)_2{\cdot}6H_2O$, and $(NH_4)_6Mo_7O_{24}{\cdot}4H_2O$, respectively, were carried out in quadruplicate under batch conditions. In each case, 2.5 g of CCF were added to 100 cm^3 of solution at an approximate concentration of 1000 ppm with respect to the metal ion in a 250 cm^3 screw-capped polypropylene bottle at 20 °C. The actual concentrations of Cd^{2+}, Co^{2+} and MoO_4^{2-} in the initial metal nitrate solutions were 919 ± 10, 738 ± 13 and 1029 ± 10 mg dm^{-3}, respectively. A control sample was also prepared in which 2.5 g of CCF were added to 100 cm^3 of deionised water. The residence times for specimens were 3, 6, 24, 48, 72 and 120 h, after which the supernatant liquors were recovered by centrifugation at 3000 rpm and simultaneously analysed for Cd, Co, Mo, Ca, Al, Si, Na, and K by inductively coupled plasma optical emission spectroscopy (ICP-OES) using a TJA Iris simultaneous ICP-OES spectrometer (TJA, MA, USA).

The kinetics of removal of Cd^{2+}, Co^{2+} and MoO_4^{2-} by CCF were modelled using the zero-, pseudo-first- and pseudo-second-order rate equations [39,40]. A zero-order reaction is described by a linear plot of concentration (q_t) versus time (t), the gradient of which gives the rate constant (k_0).

The linear form of the pseudo-first-order rate equation can be expressed as [39,40]:

$$\log(q_e - q_t) = \log q_e - k_1 t/2.303 \quad (1)$$

where k_1 (in min^{-1}) is the apparent pseudo-first-order rate constant, q_t (in mg g^{-1}) is the extent of sorption at time t (in min), and q_e (in mg g^{-1}) is the extent of sorption at equilibrium. Accordingly, the pseudo-first-order rate equation is obeyed when a linear relationship exists between $\log(q_e - q_t)$ and t, in which case, k_1 can be estimated from the gradient of the plot.

The linear form of the pseudo-second-order rate equation can be expressed as [39,40]:

$$t/q_t = 1/k_2 q_e^2 + t/q_e \quad (2)$$

where k_2 (in g mg^{-1} min^{-1}) is the apparent pseudo-second-order rate constant. In this case, estimates of k_2 and q_e can be derived from the intercept and gradient of a linear plot of t/q_t against t.

2.3. Equilibrium Removal of Cd^{2+}, Co^{2+} and MoO_4^{2-} by CCF

A preliminary evaluation indicated that equilibrium removal of Cd^{2+} and Co^{2+} by CCF was achieved within 120 h, and that of MoO_4^{2-} was established within 168 h. Thus, isotherm data were collected from single metal batch sorption experiments of varying metal concentration (10, 20, 50, 100, 200, 500, 800, 1000 and 1500 ppm) at a constant solid:solution ratio of 0.025 g dm^{-3}, following residence times of 168 h. The supernatant solutions were recovered and analysed by ICP-OES for the relevant heavy metal.

2.4. Isotherm Models

The linear form of the Langmuir isotherm, adapted for the uptake of species from solution by a solid substrate, can be represented in the following way [14,15,32]:

$$C_e/q_e = 1/q_m b + C_e/q_m \quad (3)$$

where Ce (in mg dm^{-3}) is the equilibrium concentration of the metal species in solution, q_e (in mg g^{-1}) is the amount of metal removed from solution at equilibrium, q_m (in mg g^{-1}) is the maximum sorption capacity and b (in dm^3 mg^{-1}) is the Langmuir constant. q_m and b are estimated from the intercept and the gradient of the plot of C_e/q_e against C_e.

The linear form of the Freundlich isotherm model can be expressed, thus [15,32]:

$$\log q_e = \log K_F + \log C_e/n \quad (4)$$

where K_F (in $mg^{(1-1/n)}$ $dm^{3/n}$ g^{-1}) and $1/n$ are the Freundlich constants. Favourable sorption conditions are indicated by $1/n < 1$.

2.5. Binding and Leaching of Cd^{2+}, Co^{2+} and MoO_4^{2-} from Metal-Laden CCF

An additional series of batch sorption experiments was prepared, in quadruplicate, as outlined in Section 2.1, in which 2.5 g of CCF were placed contact with the 100 cm^3 of the 1000 ppm metal solutions for 3 weeks. The metal-laden CCF samples were then recovered by sieving with a 0.5 mm mesh polypropylene sieve, washing twice with 50 cm^3 distilled water to remove loose precipitate and drying at 25 °C in air to constant mass.

Sub-samples of the metal-bearing CCF specimens were subjected to a 24-h distilled water leaching protocol [10]. The leaching procedure was carried out, in triplicate, at room temperature, at a solid:solution ratio of 0.1 g cm^{-3} and repeated four consecutive times. The leachates were analysed for the relevant heavy metal by ICP-OES and the corresponding pH values were recorded.

Triplicate sub-samples of the recovered CCF were also digested in concentrated nitric acid and the resulting liquors were analysed by ICP-OES for the relevant heavy metal. The proportions of metal species bound to CCF, present in solution and as loose precipitate, were then estimated via a mass balance for each metal.

2.6. Characterisation of Metal-Laden CCF by SEM

Secondary electron micrographs of the surfaces of gold-coated CCF samples prior to and following 3 weeks immersion in 1000 ppm metal solutions were obtained using a JEOL JSM-5310LV scanning electron microscope (JEOL (UK) Ltd, Welwyn Garden City, UK) at an accelerating voltage of 20 kV. Carbon-coated CCF surfaces and polished cross-sections were analysed by EDX using an Oxford Instruments Isis 300 X-ray microanalysis system (Oxford Instruments, Abingdon, UK). EDX maps of Ca, Si and the relevant heavy metals were acquired using characteristic Kα X-ray lines.

3. Results

3.1. Characterisation of CCF

A photograph and secondary electron SEM images of the CCF used in this study are shown in Figure 1. Approximately 50 wt% of light brown grains of flint aggregate were retained in the CCF among the grey grains of crushed cement (Figure 1a). The cement grains presented textured fracture surfaces that were littered with irregular debris (Figure 1b,c). The constituents of the cement were determined previously by differential thermal analysis to be C-S-H gel, portlandite, AFm, tetracalcium aluminate hydrate ($4CaO{\cdot}Al_2O_3{\cdot}13H_2O$) and calcite [10], which typify the composition of mature hydrated OPC.

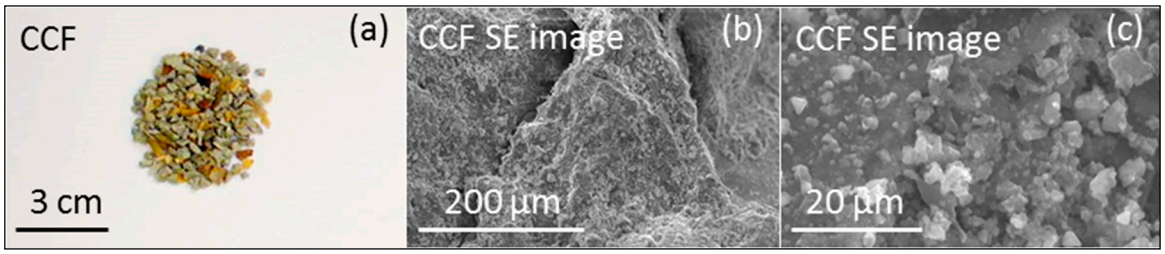

Figure 1. (**a**) Photograph of CCF, (**b**,**c**) secondary electron SEM images of the surface of CCF.

3.2. Kinetics of Removal of Cd^{2+}, Co^{2+} and MoO_4^{2-} by CCF

Figure 2 shows the extents of removal of aqueous Cd^{2+}, Co^{2+} and MoO_4^{2-} ions by CCF, and the corresponding pH profiles of the supernatant liquors are plotted in Figure 3. In all cases, small quantities of loose floc were observed to have formed in the vicinity of the CCF particles, and hence, the term 'removal' is used in favour of 'sorption' or 'uptake' in this instance. The maximum extents of removal of Cd^{2+}, Co^{2+} and MoO_4^{2-} by CCF were 36.7, 22.2 and 34.7 mg g^{-1} at 120 h, by which time equilibrium could not be confirmed. Marked increases in solution pH were observed during the removal of Cd^{2+} (from 5.47 to 11.05) and Co^{2+} (from 4.88 to 11.09); conversely, a more modest excursion in pH from 5.09 to 7.94 was recorded for the supernatant MoO_4^{2-} liquor within the 120-h timeframe (Figure 3).

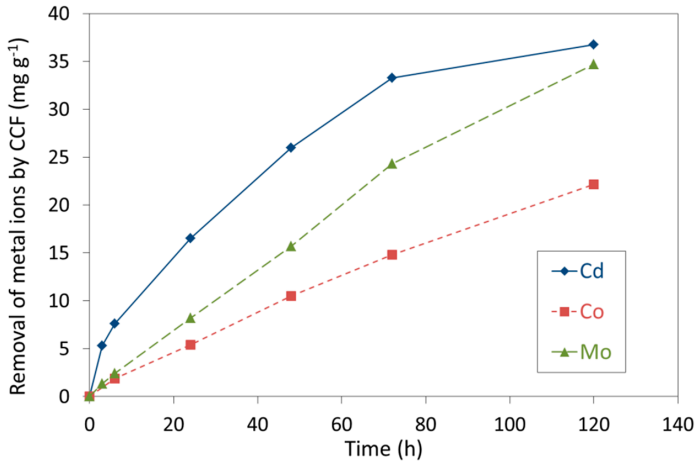

Figure 2. Removal of Cd^{2+}, Co^{2+} and MoO_4^{2-} ions by CCF.

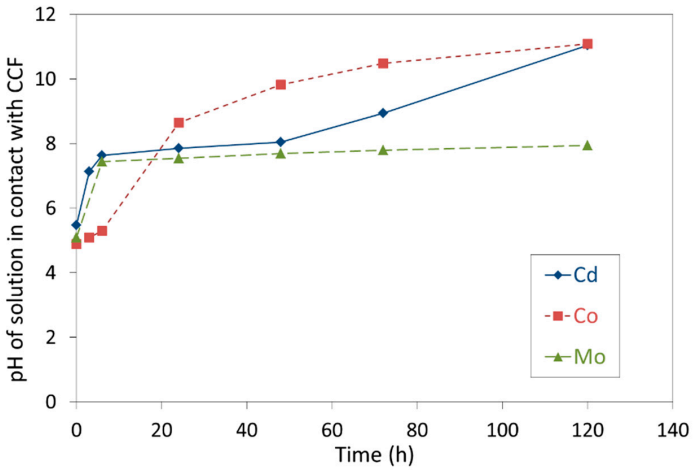

Figure 3. pH of supernatant solutions of Cd^{2+}, Co^{2+} and MoO_4^{2-} ions in contact with CCF.

The removal of the aqueous metal species by CCF was fitted to the zero-, pseudo-first- and pseudo-second-order rate models [39,40]. The apparent rate constants, k_0, k_1 and k_2, and the corresponding squares of the regression coefficients, R^2, which indicate the soundness of the correlations, are listed in Table 1. The removal of Cd^{2+} was best described by the pseudo-second-order rate equation (R^2 = 0.998); whereas, the zero-order kinetic model was found to provide the most appropriate description of the removal of Co^{2+} and MoO_4^{2-}, with R^2 values of 0.993 and 0.992, respectively.

Table 1. Kinetic parameters for the removal of Cd^{2+}, Co^{2+} and MoO_4^{2-} from aqueous solution by crushed concrete fines.

Kinetic Parameter	Cd	Co	Mo
Zero order model		-	
k_0 (mg g^{-1} min^{-1})	5.1×10^{-3}	3.1×10^{-3}	4.9×10^{-3}
R^2	0.887	0.993	0.992
Pseudo-first-order model		-	
k_1 (min^{-1})	1.0×10^{-3}	1.9×10^{-4}	3.3×10^{-4}
$q_{e\ calc.}$ (mg g^{-1})	63.6	30.6	43.5
R^2	0.881	0.985	0.945
Pseudo-second-order model		-	
k_2 (g mg^{-1} min^{-1})	2.3×10^{-5}	1.2×10^{-6}	5.1×10^{-7}
$q_{e\ calc.}$ (mg g^{-1})	38.3	61.0	114.9
R^2	0.998	0.809	0.815

The effect of extended contact between the CCF and the heavy metal solutions on the ultimate metal ion removal and dissolution of the major cement constituents was examined after 3 weeks. The exclusion of Cd^{2+} (38.7 mg g^{-1}), Co^{2+} (34.5 mg g^{-1}) and MoO_4^{2-} (34.7 mg g^{-1}) from solution and the concomitant release of calcium, sodium, potassium, aluminium and silicon are listed in Table 2. These data indicate that no further immobilisation of MoO_4^{2-} took place between 120 h and 3 weeks (Figure 2, Table 3), an additional 2.0 mg g^{-1} of Cd^{2+} removal was observed during this timeframe, and Co^{2+} exclusion from solution markedly increased by a further 12.3 mg g^{-1}.

Table 2. Metal ion removal, pH of solution and dissolution of constituents of CCF after 3 weeks.

Property [1]	Control	Cd	Co	Mo
Metal ion removal (mg g^{-1})	-	38.7	34.5	34.7
Calcium dissolution (mg g^{-1})	7.42	18.51	17.26	7.25
Sodium dissolution (mg g^{-1})	0.25	0.27	0.32	0.27
Potassium dissolution (mg g^{-1})	0.50	0.58	0.69	0.53
Aluminium dissolution (mg g^{-1})	0.13	0.06	0.01	0.14
Silicon dissolution (mg g^{-1})	0.18	0.08	0.04	0.15
pH	11.6	11.4	11.6	11.3

[1] For all samples, relative standard deviations of the concentration data were less than 5% of the mean (n = 4).

Following the 3-week contact period, the pH of the CCF control in deionised water and each of the metal-bearing supernatant solutions had increased beyond 11 by virtue of the release of alkali metal, calcium and hydroxide ions from the cement (Table 2). Calcium dissolution in the presence of Cd^{2+} and Co^{2+} was significantly more extensive than that of the control CCF sample indicating that Ca^{2+} ions from the cement were exchanged for Cd^{2+} and Co^{2+} ions from solution to some extent. Conversely, there was no significant difference between calcium dissolution of the control and that of CCF in contact with MoO_4^{2-}. Likewise, the release of silicon and aluminium species from CCF in contact with MoO_4^{2-} did not differ from that of the control sample; whereas significantly lower concentrations of Al and Si were associated with the Cd^{2+}- and Co^{2+}-bearing solutions after 3 weeks (Table 2).

Table 3. Freundlich and Langmuir isotherm parameters for the uptake of Cd^{2+}, Co^{2+} and MoO_4^{2-} from aqueous solution by crushed concrete fines.

Isotherm Parameter	Cd	Co	Mo
Langmuir model			
q_m (mg g^{-1})	45.2	38.5	24.6
b (dm^3 mg^{-1})	1.34	0.29	0.006
R^2	0.999	0.999	0.824
Freundlich model			
K_F ($mg^{(1-1/n)}$ $dm^{3/n}$ g^{-1})	21.6	11.1	0.10
$1/n$	0.169	0.235	1.255
R^2	0.639	0.784	0.991

The uptake of Cd^{2+} (14.1 mg g^{-1}), Co^{2+} (14.7 mg g^{-1}) and MoO_4^{2-} (15.5 mg g^{-1}) by direct binding to CCF after 3 weeks was determined by nitric acid digestion of the recovered metal-laden solids (following the removal of the loose floc precipitate by washing). The final partition of each metal ion between the CCF, loose floc and solution is plotted in Figure 4. In excess of 99.9% of the Cd^{2+} and Co^{2+} present in the initial solutions were removed during contact with CCF, although only 38.3 and 49.9%, respectively, were bound to CCF, with the remainder having precipitated as floc. MoO_4^{2-} was less efficiently excluded from solution with 8.6% remaining in the aqueous phase after 3 weeks; although, the extent of binding to CCF, 41.2%, was intermediate between those of Cd^{2+} and Co^{2+} (Figure 4).

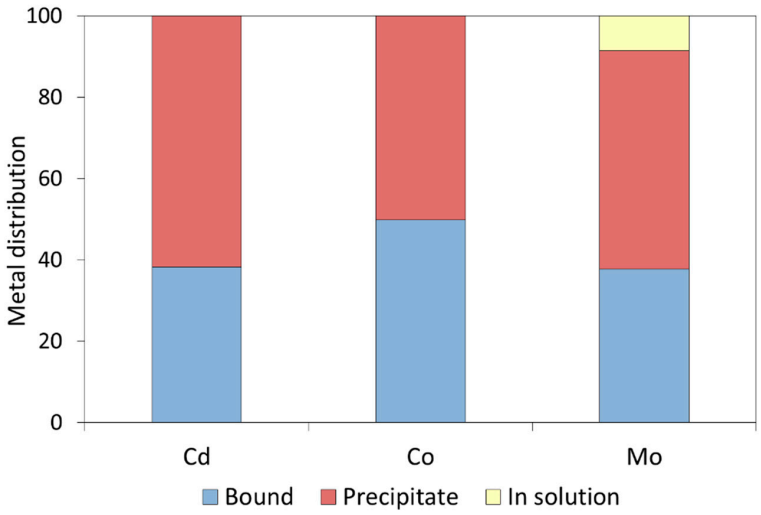

Figure 4. The final partition of each metal after 3 weeks.

3.3. Isotherm Models of Equilibrium Removal of Cd^{2+}, Co^{2+} and MoO_4^{2-} by CCF

Isotherms of the equilibrium uptake of Cd^{2+}, Co^{2+} and MoO_4^{2-} by CCF plotted against the final equilibrium solution concentration are presented in Figure 5. The maximum observed extents of removal of Cd^{2+}, Co^{2+} and MoO_4^{2-} were found to be 45.2, 38.4 and 56.0 mg g^{-1}, respectively, at an initial solution concentration of 1500 ppm (Figure 5).

The equilibrium removal data for Cd^{2+} and Co^{2+} were found to correlate well with the Langmuir model (R^2 = 0.999 in both cases) for which the theoretical maximum removal capacities were within 1% of the experimentally determined values (Table 3, Figure 5). Conversely, the Freundlich model was found to provide a more appropriate description of the immobilisation of MoO_4^{2-} ions (R^2 = 0.991).

Since the removal of Cd^{2+}, Co^{2+} and MoO_4^{2-} in the presence of CCF occurs by a combination of binding and precipitation, the Langmuir and Freundlich constants cannot be used to indicate the energetics of these sorption processes. Nonetheless, these models

provide a useful description of the maximum equilibrium capacity of the CCF to exclude the metal species from solution.

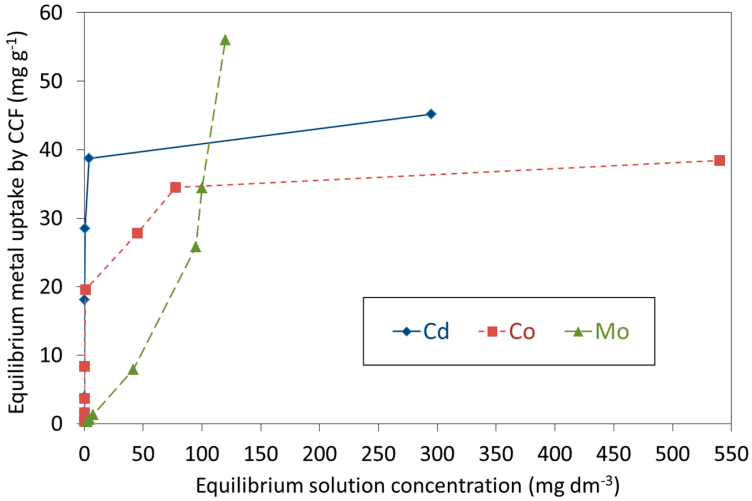

Figure 5. Equilibrium isotherm plots of the uptake of Cd^{2+}, Co^{2+} and MoO_4^{2-} ions by CCF as a function of final metal ion concentration of the supernatant solution.

3.4. The Fate of the Cd^{2+}, Co^{2+} and MoO_4^{2-} Species Bound to CCF

Secondary electron SEM images of the surfaces of the metal-laden CCF particles following exposure to 1000 ppm Cd^{2+}, Co^{2+} and MoO_4^{2-} solutions for 3 weeks (viz. Cd-CCF, Co-CCF and Mo-CCF, respectively) are shown in Figure 6. The relative concentrations of the major elements of the metal-bearing structures formed on the CCF surfaces were determined by EDX analysis and are listed in Table 4. It should be noted that, owing to the intimacy of the various phases on the surface of the CCF particles, EDX data for any given structure is likely to be "contaminated" by signals arising from neighbouring phases.

The surface of Cd-CCF was characterised by a cadmium-bearing calcium aluminosilicate cancellated network (Cd:Ca = 1.0:1.12) upon which were deposited calcium-rich platy foils (Cd:Ca = 1.0:10.4) which are tentatively considered to be newly formed precipitates of Cd-substituted portlandite (Figure 6, Table 4). A back-scattered electron image of a cross-section through the surface of a Cd-CCF particle and corresponding EDX maps for cadmium, calcium and silicon are shown in Figure 7. These images indicate that the principal mechanisms of uptake of cadmium by CCF were the initial formation of the cadmium-bearing cancellated network and the subsequent precipitation of the Cd-substituted platy crystals. The EDX mapping also demonstrates that there was no appreciable diffusion of cadmium ions into the interior of the cement matrix (Figure 7).

Table 4. Composition of metal-bearing structures on the surface of CCF.

Structure	Relative Elemental Composition (Moles per Mole of Al) [1]			
	Al	Si	Ca	Metal ion
Cd-CCF				
Cancellated network	1.00 ± 0.29	2.52 ± 0.12	6.45 ± 0.24	5.38 ± 1.12
Platy foils	1.00 ± 0.41	4.28 ± 1.20	99.9 ± 5.2	9.59 ± 2.85
Co-CCF				
Foliaceous network	1.00 ± 0.12	0.93 ± 0.15	146.0 ± 0.8	7.17 ± 1.35
Fluffy pom-poms	1.00 ± 0.08	2.72 ± 0.29	1.32 ± 0.12	56.65 ± 0.91
Mo-CCF				
Peloids	1.00 ± 1.07	2.91 ± 2.32	34.03 ± 7.13	36.07 ± 3.41
Distorted polygons	1.00 ± 0.13	4.60 ± 0.24	131.1 ± 9.5	34.81 ± 6.7

[1] Composition data are normalised relative to the proportion of aluminium present.

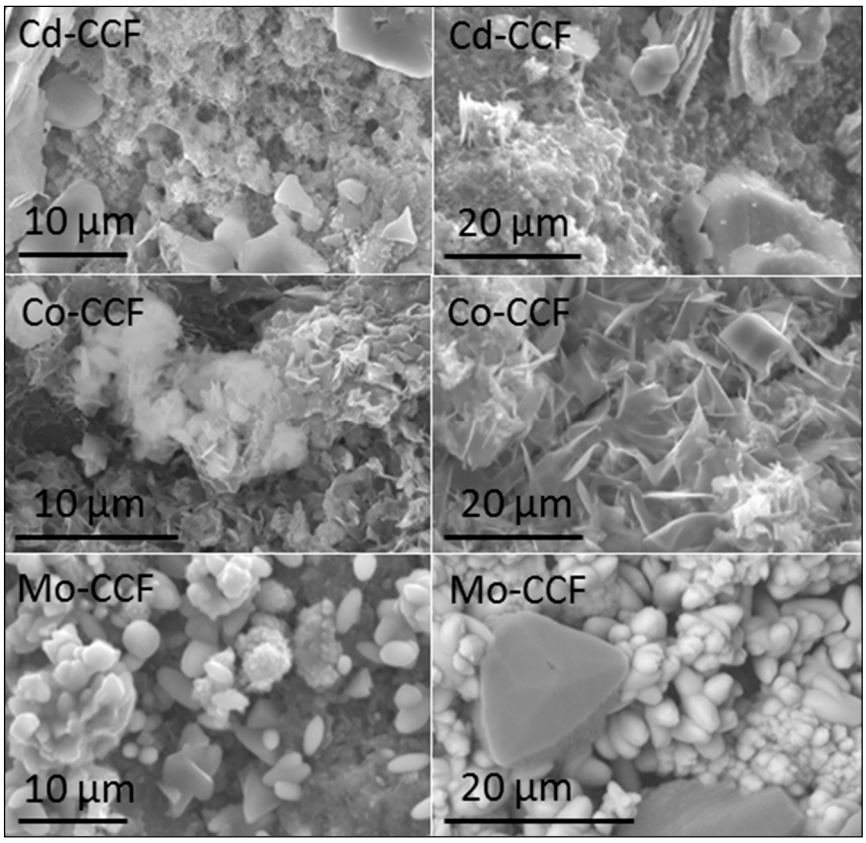

Figure 6. Secondary electron images depicting the surfaces of cadmium-laden CCF (Cd-CCF) showing a cadmium-bearing cancellated network and platy foils; cobalt-laden CCF (Co-CCF) showing cobalt-rich fluffy pom-pom structures and a foliaceous network; molybdenum-laden CCF (Mo-CCF) showing molybdenum-rich peloids and occasional distorted polygons.

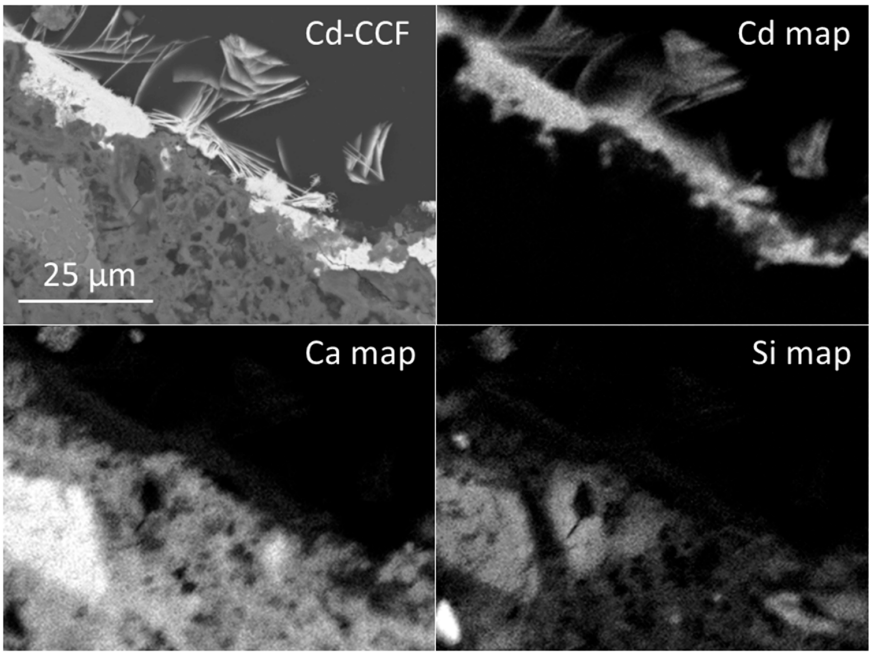

Figure 7. Back-scattered electron micrograph of cross section of cadmium-laden CCF particle and corresponding EDX maps for cadmium, calcium and silicon. All images are of the same sample area.

Cobalt-rich fluffy pom-pom structures (Co:Ca = 43.0:1.0) and a cobalt-bearing foliaceous network (Co:Ca = 1.0:20.4) are observed in the secondary electron images of the Co-CCF surfaces ((Figure 6, Table 4). Two distinct cobalt-bearing layers are also noted in the corresponding back scattered electron image and cobalt EDX map of a cross-section through the surface of Co-CCF (Figure 8). This demonstrates that Co^{2+} ions were bound by a two-stage precipitation process with no significant penetration of Co^{2+} species into the cement matrix.

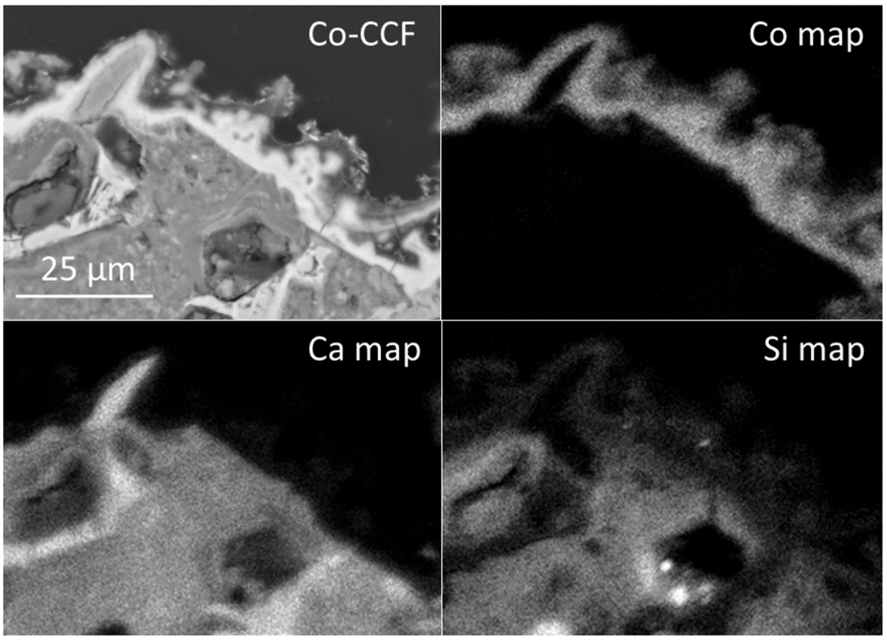

Figure 8. Back-scattered electron micrograph of cross section of cobalt-laden CCF particle and corresponding EDX maps for cobalt, calcium and silicon. All images are of the same sample area.

The surface of Mo-CCF was found to be extensively populated with a mass of molybdenum-rich (1–10 µm) peloids (Mo:Ca = 1.1:1.0), whose stoichiometry suggests that they may be powellite ($CaMoO_4$), intermixed with occasional larger (~20 µm) distorted polygons (Mo:Ca = 1.0:3.8) (Figure 6, Table 4). The back scattered electron image of Mo-CCF and corresponding EDX maps confirm the superficial formation of the calcium molybdenate precipitates and also demonstrate that the diffusion of molybdenum species into the cement matrix was negligible (Figure 9).

3.5. Leaching of Cd^{2+}, Co^{2+} and MoO_4^{2-} Species Bound to CCF

Figure 10 shows the cumulative concentration of heavy metal species leached from Cd-CCF, Co-CCF and Mo-CCF after four consecutive leaching procedures with distilled water. The corresponding pH values of the leachate solutions were between 9.8 and 10.7 indicating that the reserve of soluble alkaline constituents of the cement persisted throughout the 3-week duration of contact with the metal solutions and during the four successive 24-h leach tests. The proportions of the heavy metals leached relative to the bound quantities were 5.8, 4.6 and 2.4% for Cd-CCF, Co-CCF and Mo-CCF, respectively (Figure 10).

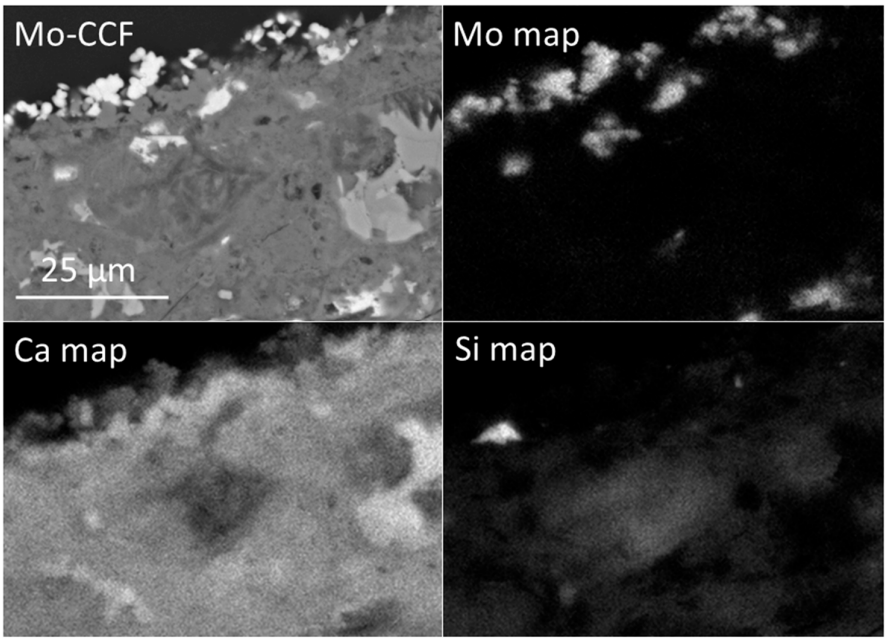

Figure 9. Back-scattered electron micrograph of cross section of molybdenum-laden CCF particle and corresponding EDX maps for molybdenum, calcium and silicon. All images are of the same sample area.

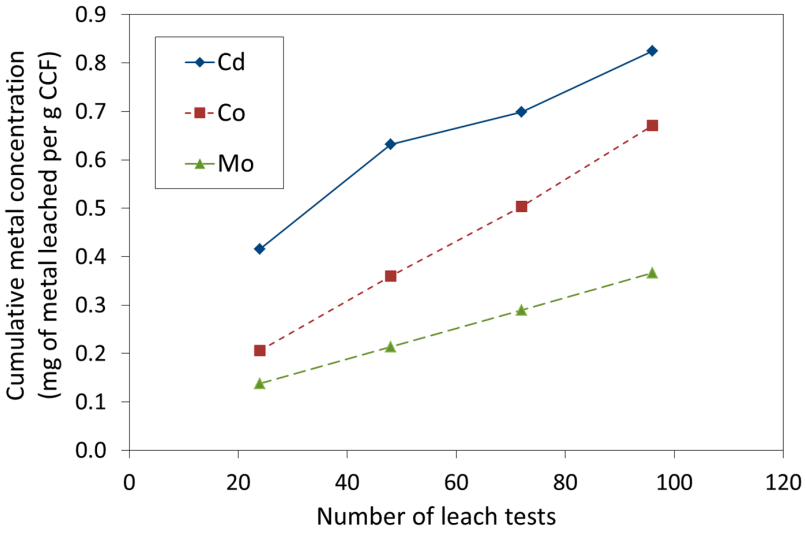

Figure 10. Cumulative concentration of metal species in distilled water leachate.

4. Discussion

In light of the failure to effectively recycle or reutilise the vast quantities of concrete-based C&D waste, further research into the potential use of the cement-rich fine fraction as a sorbent for aqueous heavy metal contaminants has been suggested [7,11]. Accordingly, the present study was carried out to investigate the interactions of aqueous Cd^{2+}, Co^{2+} and MoO_4^{2-} ions with crushed concrete fines.

The 5-year laboratory-prepared CCF used in this study have been shown to remove 45.2, 38.4 and 56.0 mg g^{-1} of Cd^{2+}, Co^{2+} and MoO_4^{2-}, respectively, under steady state conditions from single metal nitrate solutions of up to 1500 ppm (Figure 5). The equilibrium uptakes of Cd^{2+}, Co^{2+} and MoO_4^{2-} by CCF are compared with those of other cement-based and inorganic sorbents in Table 5 [5,6,13–15,32,40–48]. The removal capacity of CCF for Co^{2+} and MoO_4^{2-} was found to be superior to those of other sorbents reported in the

literature; whereas the uptake of Cd^{2+} appeared in the middle of the range (Table 5). In general, equilibration times for the removal of aqueous metal species by calcium silicate-based inorganic sorbents, involving lattice substitution and co-precipitation mechanisms, tend to be appreciably longer (24 h or more) than those of polymeric organic sorbents, such as chitosan, for which steady state uptake by ion-exchange with functional groups can often be achieved within minutes [49–51]. Lack of kinetic efficiency can limit the potential industrial wastewater treatment applications of sorbents, particularly CCF, whose equilibration times for the removal of Cd^{2+} (120 h), Co^{2+} (120 h) and MoO_4^{2-} (168 h) are typically longer than those of other calcium silicates [42–44].

Table 5. Comparison of the removal characteristics of CFF for Cd^{2+}, Co^{2+} and MoO_4^{2-} with those of other crushed concretes and inorganic sorbents.

Sorbent	[1] C_i Range (ppm)	Solid:Liquid Ratio (mg cm^{-3})	[2] q_m (mg g^{-1})	[3] t_{eq} (min)	Ref.
Cadmium, Cd^{2+}					
Laboratory CCF	10–1500	25	45.2	7200	This study
Laboratory CCF	0.4–4.0	25	0.294	1440	[14]
Laboratory autoclaved CCF	0–5000	100	15	1440	[15]
NaOH-pretreated CCF	5–200	1	0.61	1440	[13]
Waste-derived tobermorite	5.6–124	0.25	179	8640	[32]
Waste dolomite	500–2000	20–80	89.9	45	[41]
Blast furnace slag	0–5	0.1–20	5.1	1440	[42]
Coal fly ash	0–5	0.1–20	3.8	1440	[42]
Cobalt, Co^{2+}					
Laboratory CCF	10–1500	25	38.4	7200	This study
Demolition CCF	5.9–471	5	18.9	1440	[5,6]
Waste-derived tobermorite	0–100	50	10.47	7200	[40]
Waste-derived calcium silicate	200	2.5	78	>300	[43]
Red mud	5.9–354	5	30.6	1440	[44]
Molybdenum, MoO_4^{2-}					
Laboratory CCF	10–1500	25	56.0	10,080	This study
Waste Fe/Mn hydroxides	48	10	4.4	1440	[45]
Synthetic goethite	0–19	0.3	15.5	1020	[46]
Zeolite-supported Fe_3O_4	0.1–5	0.025–0.5	17.92	1440	[47]
Modified montmorillonite	4798	20	37.2	1440	[48]

[1] C_i = initial metal concentration in solution. [2] q_m = maximum metal uptake. [3] t_{eq} = time to equilibrium.

As mentioned previously, the immobilisation of heavy metal species incorporated into freshly mixed Portland cement can take place via a range of mechanisms, including ion-exchange and isomorphic substitution, chemi- and physisorption, and the pH-mediated precipitation of solubility limiting phases [10,31,38]. In this study, all three metal species were found to be excluded from solution by co-precipitation onto, and in the vicinity of, the surface of the CCF particles with no detectible diffusion into the existing phases of the mature cement matrix (Figures 7–9).

A recent study has demonstrated that MoO_4^{2-} ions can substitute into pre-existing AFm and AFt phases and also electrostatically sorb to the C-S-H gel phase at very low concentrations (<5 μM) with long equilibration times of up to 30 days [38]. Under the same experimental parameters, MoO_4^{2-} ions were found to re-precipitate in the presence of portlandite to form the solubility limiting powellite, $CaMoO_4$, phase [38]. It is likely that the markedly higher concentration (1000 ppm) of MoO_4^{2-} ions used in the present study favoured the precipitation of powellite on the surface of the CCF particles, thus mitigating the slower diffusion of MoO_4^{2-} into the cement matrix. Investigations of the fate of Cd^{2+} and Co^{2+} in contact with crushed concrete-based materials could not be found in the current literature for comparison with the present findings that these metal ions are also exclusively immobilised by precipitation.

Kinetics of removal of Co^{2+} and MoO_4^{2-} ions, in the presence of CCF, approximated to a zero-order reaction indicating that the rates of immobilisation of the metal species were independent of their concentrations (Table 1). In these cases, the rates of precipitation were presumably controlled by the availability of Ca^{2+} ions involved in the co-precipitation processes. Conversely, the removal of Cd^{2+} was found to follow a pseudo-second order rate ($k_2 = 2.3 \times 10^{-5}$ g mg^{-1} min^{-1}), which is in close agreement with the findings of Kumara et al. [15] for the uptake of Cd^{2+} by crushed concrete fines ($k_2 = 3 \times 10^{-5}$ g mg^{-1} min^{-1}).

The equilibrium removal of Cd^{2+} and Co^{2+} by CCF reached a plateau at an initial metal ion concentration of 1000 ppm and conformed to the Langmuir model (Table 3, Figure 5). This compares well with the work of Damrongsiri [14], Kumara et al. [15] and Shin et al. [13] who successfully used the Langmuir model to describe the uptake of Cd^{2+} ions by various cement-based fines. Šljivić-Ivanović et al. [5] also report a Langmuir-type curve with a plateau for the uptake of Co^{2+} ions by crushed concrete demolition waste, although they did not model the data.

The removal of MoO_4^{2-} ions by CCF did not reach a plateau and was best described by the Freundlich isotherm (Table 3, Figure 5). It is considered that the persistent reserves of soluble Ca^{2+} ions from the CCF continued to effect the precipitation of increasing quantities of powellite as the initial solution concentration was increased from 10 to 1500 ppm.

Despite the high sorption capacity of CCF for Cd^{2+}, Co^{2+} and MoO_4^{2-}, the slow removal kinetics, exceptionally long equilibration times, floc formation and high pH are likely to limit their use as sorbents in many conventional wastewater treatment applications. Nonetheless, these characteristics, along with the persistent binding of the precipitated metals under successive leaching, may be usefully exploited in the management of metal contaminants in soils, sediments and groundwater. In this respect, their incorporation into reactive barriers could be used to conserve other natural geo-sorbents such as clays and zeolites.

5. Conclusions

In this study, single metal batch sorption experiments confirmed that crushed concrete fines (CCF) were an effective sorbent for the removal of Cd^{2+} (45.2 mg g^{-1}), Co^{2+} (38.4 mg g^{-1}) and MoO_4^{2-} (56.0 mg g^{-1}) ions from aqueous solutions. The principal mechanism of sorption was co-precipitation with Ca^{2+} ions released from the cement to form solubility limiting phases, and some loose metal-bearing floc was also observed to have formed. Four consecutive distilled water leach tests indicated that less than 6% of each sorbed heavy metal was readily leachable. The Langmuir model provided the most appropriate description of the steady state immobilisation of Cd^{2+} and Co^{2+}, whereas the removal of MoO_4^{2-} conformed to the Freundlich isotherm. Long equilibration times (>120 h), loose floc formation and high pH are likely to limit the use of CCF in many conventional wastewater treatment applications; although, these properties could be usefully exploited in reactive barriers for the management of contaminated soils, sediments and groundwater.

Author Contributions: Conceptualization, N.J.C.; methodology, N.J.C. and V.K.E.; software, N.J.C.; validation, N.J.C. and V.K.E.; formal analysis, N.J.C. and V.K.E.; investigation, N.J.C. and V.K.E.; resources, N.J.C.; data curation, N.J.C.; writing—original draft preparation, N.J.C.; writing—review and editing, V.K.E.; visualization, N.J.C.; supervision, N.J.C.; project administration, N.J.C.; funding acquisition, N.J.C. All authors have read and agreed to the published version of the manuscript.

Funding: This research received no external funding.

Acknowledgments: The authors acknowledge, with gratitude, the technical support provided by Ian Slipper for the collection of the SEM and EDX; also Christine Dimech for the collection of some of the ICP data.

Conflicts of Interest: The authors declare no conflict of interest.

References

1. Jelić, I.V.; Sljivic-Ivanovic, M.; Dimović, S.D.; Antonijević, D.L.; Jovic, M.; Vujović, Z.; Smiciklas, I. Radionuclide Immobilization by Sorption onto Waste Concrete and Bricks—Experimental Design Methodology. *Water Air Soil Pollut.* **2019**, *230*, 242. [CrossRef]
2. Zimbili, O.; Salim, W.; Ndambuki, M. A review on the usage of ceramic wastes in concrete production. *Int. J. Civ. Archit. Struct. Constr. Eng.* **2014**, *8*, 91–95.
3. Chen, Q.; Lan, Q.; Li, X.; Zhou, J.; Yang, Z.; Zhou, Y. Utilization of fine powder in demolition concrete as recyclable coagulant in removing color from dye-bearing wastewater. *Environ. Earth Sci.* **2015**, *74*, 6737–6745. [CrossRef]
4. Kucukvar, M.; Eğilmez, G.; Tatari, O. Evaluating environmental impacts of alternative construction waste management approaches using supply-chain-linked life-cycle analysis. *Waste Manag. Res.* **2014**, *32*, 500–508. [CrossRef]
5. Sljivic-Ivanovic, M.; Jelić, I.V.; Dimovic, S.; Antonijević, D.L.; Jovic, M.; Mraković, A.; Smiciklas, I. Exploring innovative solutions for aged concrete utilization: Treatment of liquid radioactive waste. *Clean Technol. Environ. Policy* **2018**, *20*, 1343–1354. [CrossRef]
6. Jelić, I.; Šljivić-Ivanović, M.; Dimović, S.; Antonijević, D.; Jović, M.; Mirković, M.; Smičiklas, I. The applicability of construction and demolition waste components for radionuclide sorption. *J. Clean. Prod.* **2018**, *171*, 322–332. [CrossRef]
7. Grace, M.A.; Clifford, E.; Healy, M.G. The potential for the use of waste products from a variety of sectors in water treatment processes. *J. Clean. Prod.* **2016**, *137*, 788–802. [CrossRef]
8. EU Construction and Demolition Waste Protocol and Guidelines. Available online: https://ec.europa.eu/growth/content/eu-construction-and-demolition-waste-protocol-0_en (accessed on 10 January 2020).
9. EPA Sustainable Management of Construction and Demolition Materials. Available online: https://www.epa.gov/smm/sustainable-management-construction-and-demolition-materials. (accessed on 29 December 2020).
10. Coleman, N.J.; Lee, W.E.; Slipper, I.J. Interactions of aqueous Cu, Zn and Pb ions with crushed concrete fines. *J. Hazard. Mater.* **2005**, *121*, 203–213. [CrossRef]
11. Kumara, G. Reviews on the applicability of construction and demolition waste as low-cost adsorbents to remove-heavy metals in wastewater. *Int. J.* **2018**, *14*, 44–51. [CrossRef]
12. Shin, W.-S.; Kim, Y.-K. Removal Characteristics of Heavy Metals from Aqueous Solution by Recycled Aggregate and Recycled Aggregate/Steel Slag Composites as Industrial Byproducts. *Appl. Chem. Eng.* **2015**, *26*, 477–482. [CrossRef]
13. Shin, W.-S.; Na, K.-R.; Kim, Y.-K. Adsorption of metal ions from aqueous solution by recycled aggregate: Estimation of pretreatment effect. *Desalin. Water Treat.* **2015**, *57*, 9366–9374. [CrossRef]
14. Damrongsiri, S. Feasibility of using demolition waste as an alternative heavy metal immobilising agent. *J. Environ. Manag.* **2017**, *192*, 197–202. [CrossRef] [PubMed]
15. Kumara, G.M.P.; Kawamoto, K.; Saito, T.; Hamamoto, S.; Asamoto, S. Evaluation of Autoclaved Aerated Concrete Fines for Removal of Cd(II) and Pb(II) from Wastewater. *J. Environ. Eng.* **2019**, *145*, 04019078. [CrossRef]
16. Ali, A.F.; Ali, Z.T.A. Removal of lead ions from wastewater using crushed concrete demolition waste. *Assoc. Arab. Univ. J. Eng. Sci.* **2019**, *26*, 22–29. [CrossRef]
17. Ali, A.F.; Ali, Z.T.A. Interaction of Aqueous Cu2+ Ions with Granules of Crushed Concrete. *Iraqi J. Chem. Pet. Eng.* **2019**, *20*, 31–38. [CrossRef]
18. Yoo, J.; Shin, H.; Ji, S. Evaluation of the Applicability of Concrete Sludge for the Removal of Cu, Pb, and Zn from Contaminated Aqueous Solutions. *Metals* **2018**, *8*, 666. [CrossRef]
19. Kittnerová, J.; Drtinová, B.; Štamberg, K.; Vopálka, D.; Evans, N.; Deissmann, G.; Lange, S. Comparative study of radium and strontium behaviour in contact with cementitious materials. *Appl. Geochem.* **2020**, *122*, 104713. [CrossRef]
20. Liu, C.; Yang, Y.; Wan, N. Kinetic studies of phosphate adsorption onto construction solid waste (CSW). *Water Qual. Res. J.* **2014**, *49*, 307–318. [CrossRef]
21. Egemose, S.; Sønderup, M.J.; Beinthin, M.V.; Reitzel, K.; Hoffmann, C.C.; Flindt, M.R. Crushed Concrete as a Phosphate Binding Material: A Potential New Management Tool. *J. Environ. Qual.* **2012**, *41*, 647–653. [CrossRef]
22. Wu, L.; Tang, J.; Zhang, S.; Wang, J.; Ding, X. Using Recycled Concrete as an Adsorbent to Remove Phosphate from Polluted Water. *J. Environ. Qual.* **2019**, *48*, 1489–1497. [CrossRef]
23. Dos Reis, G.S.; Cazacliu, B.G.; Correa, C.R.; Ovsyannikova, E.; Kruse, A.; Sampaio, C.H.; Lima, E.C.; Dotto, G.L. Adsorption and recovery of phosphate from aqueous solution by the construction and demolition wastes sludge and its potential use as phosphate-based fertiliser. *J. Environ. Chem. Eng.* **2020**, *8*, 103605. [CrossRef]
24. Kim, Y.-K.; Shin, W.-S. Effects of Capping with Recycled Aggregates and Natural Zeolite on Inhibition of Contaminants Release from Marine Sediment. *J. Korean Soc. Water Environ.* **2016**, *32*, 546–551. [CrossRef]
25. Kang, K.; Lee, C.-G.; Choi, J.-W.; Kim, Y.-K.; Park, S.-J. Evaluation of the Use of Sea Sand, Crushed Concrete, and Bentonite to Stabilize Trace Metals and to Interrupt Their Release from Contaminated Marine Sediments. *Water Air Soil Pollut.* **2016**, *227*, 308. [CrossRef]
26. Shin, W.; Kim, Y.-K. Stabilization characteristics of metal ions in marine-contaminated sediments by recycled aggregate. *J. Soils Sediments* **2017**, *17*, 1806–1814. [CrossRef]
27. Ali, A.F.; Ali, Z.T.A. Sustainable Use of Concrete Demolition Waste as Reactive Material in Permeable Barrier for Remediation of Groundwater: Batch and Continuous Study. *J. Environ. Eng.* **2020**, *146*, 04020048. [CrossRef]
28. Wang, Y.; Sikora, S.; Townsend, T.G. Ferrous iron removal by limestone and crushed concrete in dynamic flow columns. *J. Environ. Manag.* **2013**, *124*, 165–171. [CrossRef] [PubMed]

29. Gartner, E.M.; Young, J.F.; Damidot, D.A.; Jawed, I. Hydration of Portland cement. In *Structure and Performance of Cements*, 2nd ed.; Bensted, J., Barnes, P., Eds.; Spon Press: London, UK, 2002; pp. 57–113.
30. Tchounwou, P.B.; Yedjou, C.G.; Patlolla, A.K.; Sutton, D.J. Heavy Metal Toxicity and the Environment. *Exp. Suppl.* **2012**, *101*, 133–164. [CrossRef]
31. Evans, N. Binding mechanisms of radionuclides to cement. *Cem. Concr. Res.* **2008**, *38*, 543–553. [CrossRef]
32. Coleman, N.J. Interactions of Cd(II) with waste-derived 11Å tobermorites. *Sep. Purif. Technol.* **2006**, *48*, 62–70. [CrossRef]
33. Donaldson, J.D.; Beyersmann, D. Cobalt and Cobalt Compounds. In *Ullmann's Encyclopedia of Industrial Chemistry*; Wiley: Weinheim, Germany, 2005.
34. Garcia, M.D.; Hur, M.; Chen, J.J.; Bhatti, M.T. Cobalt toxic optic neuropathy and retinopathy: Case report and review of the literature. *Am. J. Ophthalmol. Case Rep.* **2020**, *17*, 100606. [CrossRef]
35. Vespa, M.; Dähn, R.; Grolimund, D.; Wieland, E.; Scheidegger, A.M.; Dähn, R. Co Speciation in Hardened Cement Paste: A Macro- and Micro-Spectroscopic Investigation. *Environ. Sci. Technol.* **2007**, *41*, 1902–1908. [CrossRef] [PubMed]
36. Mitchell, P.C.H.; Outteridge, T.; Kloska, K.; McMahon, S.; Epshteyn, Y.; Sebenik, R.F.; Burkin, A.R.; Dorfler, R.R.; Laferty, J.M.; Leichtfried, G.; et al. Molybdenum and Molybdenum Compounds. In *Ullmann's Encyclopedia of Industrial Chemistry*, 7th ed.; Elvers, B., Ed.; Wiley-VCH: Weinheim, Germany, 2020. [CrossRef]
37. Turnlund, J.R.; Friberg, L.T. Molybdenum. In *Handbook of the Toxicology of Metals*, 3rd ed.; Nordberg, G.F., Fowler, B.A., Nordberg, M., Friberg, L.T., Eds.; Academic Press: Cambridge, MA, USA, 2007; pp. 731–741. [CrossRef]
38. Lange, S.; Klinkenberg, M.; Barthel, J.; Bosbach, D.; Deissmann, G. Uptake and retention of molybdenum in cementitious systems. *Appl. Geochem.* **2020**, *119*, 104630. [CrossRef]
39. Ho, Y.; McKay, G. The sorption of lead(II) ions on peat. *Water Res.* **1999**, *33*, 578–584. [CrossRef]
40. Coleman, N.J.; Brassington, D.S.; Raza, A.; Mendham, A.P. Sorption of Co^{2+} and Sr^{2+} by waste-derived 11 Å tobermorite. *Waste Manag.* **2006**, *26*, 260–267. [CrossRef] [PubMed]
41. Gruszecka-Kosowska, A.; Baran, P.; Wdowin, M.; Franus, W. Waste dolomite powder as an adsorbent of Cd, Pb(II), and Zn from aqueous solutions. *Environ. Earth Sci.* **2017**, *76*, 521. [CrossRef]
42. Nguyen, T.C.; Loganathan, P.; Nguyen, T.V.; Kandasamy, J.; Naidu, R.; Vigneswaran, S. Adsorptive removal of five heavy metals from water using blast furnace slag and fly ash. *Environ. Sci. Pollut. Res.* **2017**, *25*, 20430–20438. [CrossRef]
43. Yarusova, S.; Gordienko, P.S.; Yudakov, A.A.; Azarova, Y.A.; Yashchuk, R.D. Kinetics of the sorption of heavy-metal ions by a sorbent obtained from boric acid production waste. *Theor. Found. Chem. Eng.* **2016**, *50*, 841–845. [CrossRef]
44. Milenkovic, A.; Smiciklas, I.; Markovic, J.; Vukelic, N. Immobilization of 60Co and 90Sr ions using red mud from aluminum industry. *Nucl. Technol. Radiat. Prot.* **2014**, *29*, 79–87. [CrossRef]
45. Vaziyeva, A.; Pavlenko, O. Investigation of molybdate ion sorption on the sorbent from industrial waste. *Chem. Chem. Technol.* **2017**, *11*, 291–295. [CrossRef]
46. Xu, N.; Christodoulatos, C.; Braida, W. Modeling the competitive effect of phosphate, sulfate, silicate, and tungstate anions on the adsorption of molybdate onto goethite. *Chemosphere* **2006**, *64*, 1325–1333. [CrossRef]
47. Verbinnen, B.; Block, C.; Hannes, D.; Lievens, P.; Vaclavikova, M.; Stefusova, K.; Gallios, G.; Vandecasteele, C. Removal of Molybdate Anions from Water by Adsorption on Zeolite-Supported Magnetite. *Water Environ. Res.* **2012**, *84*, 753–760. [CrossRef] [PubMed]
48. Andrunik, M.; Muir, B.; Kowalik, M.; Socha, R.P.; Bajda, T. Sorption of Molybdates and Tungstates on Functionalized Montmorillonites: Structural and Textural Features. *Materials* **2019**, *12*, 2253. [CrossRef]
49. Lemrabet, E.; Jaafari, K.; Benkhouja, K.; Touaiher, M.; Bakasse, M.; Sahraoui, B.; Touhtouh, S.; Soufiane, A. Removal of heavy-metal ion by adsorption on chitosan gel beads. *J. Optoelectron. Adv. Mater.* **2013**, *15*, 1298–1302.
50. Brion-Roby, R.; Gagnon, J.; Nosrati, S.; Deschênes, J.-S.; Chabot, B. Adsorption and desorption of molybdenum(VI) in contaminated water using a chitosan sorbent. *J. Water Process. Eng.* **2018**, *23*, 13–19. [CrossRef]
51. Kumar, R.; Chawla, J. Removal of Cadmium Ion from Water/Wastewater by Nano-metal Oxides: A Review. *Water Qual. Expo. Health* **2013**, *5*, 215–226. [CrossRef]